PERGAMON

Journal of Structural Geology 22 (2000) 1049–1064

JOURNAL OF STRUCTURAL GEOLOGY

www.elsevier.nl/locate/jstrugeo

Plio-Quaternary paleostress regimes and relation to structural development in the Kertch–Taman peninsulas (Ukraine and Russia)

Aline Saintot[a,*], Jacques Angelier[b]

[a]*Vrije Universiteit, Instituut voor Aardwetenschappen, De Boelelaan, 1085, 1081HV, Amsterdam, The Netherlands*
[b]*Laboratoire de Tectonophysique, Département de Géotectonique, U.P.R.E.S.A. 7072, U.P.M.C., Tr 25–26, E1, case 129, 4 Place Jussieu, 75252 Paris cedex 05, France*

Received 12 August 1998; accepted 17 March 2000

Abstract

In the Kertch–Taman peninsulas, located between the Crimean and NW-Caucasus Mountains, deep troughs developed since Oligocene time. Sediments were subsequently folded. Folding was associated with thrusting. Paleostress analyses allowed constraint of the tectonic evolution of the area. An extensional event occurred before folding, perhaps related to the trough development. This event was followed by compression associated with Plio-Quaternary folding. Stress tensors determined in older rocks in the Crimean and NW-Caucasus belts are correlated with this regional Plio-Quaternary compression. In detail, N–S compression followed NW–SE compression. This change in direction could be explained by a change of the direction of convergence of the Black Sea Plate with the Scythian Plate. The NW–SE compression induced NE–SW folds in the southern part of the peninsulas. The N–S compression corresponds to E–W folds of the northern part, suggesting a northward propagation of the deformation front. The structural evolution of the Kertch–Taman region is controlled by (1) pre-existing structures, (2) a change in the direction of compression related to a change of the direction of convergence of the Black Sea with the Scythian Plate and (3) the northward propagation of the compressional front with the continuing indentation of the Black Sea block.

1. Introduction

Crimea and Caucasus belong to the same major Alpine mountain belt (Muratov and Tseisler, 1978; Zonenshain et al., 1990; Milanovsky, 1991, 1996), even though there are numerous differences in their specific stratigraphic and structural histories (Muratov et al., 1984). The Kertch–Taman peninsulas are an area of subsidence located between the Black Sea and the Azov Sea, and separate the Crimean Mountains and the NW-Caucasus fold-and-thrust belt, forming a huge along-strike saddle (Fig. 1). This area is characterised by a very thick Cenozoic terrigeneous sequence that overlies and masks the axial zone of the Crimea–NW-Caucasus belt. This sequence shows numerous folds and alignments of mud volcanoes.

In addition to some outcrops in the interior of the Kertch–Taman peninsulas, shoreline cliffs provide magnificent exposures and cross-sections. For this reason, numerous stratigraphic features of the eastern Para-Tethys were defined in this area. The most commonly accepted equivalences between the well-known Mediterranean stratigraphic epochs and the regional definitions are given on Fig. 2.

The structural development of this region is controversial, especially regarding the origin of anticlines and mud volcanoes. According to some authors, diapiric mechanisms suffice to explain development of non-cylindrical anticlines and crestal mud volcanoes (Gri-

* Corresponding author.
E-mail addresses: saia@geo.vu.nl (A. Saintot), ja@lgs.jussieu.fr (J. Angelier).

0191-8141/00/$ - see front matter
PII: S0191-8141(00)00025-0

gor'yants et al., 1981). Muratov and Tseisler (1978) assumed that folding was associated with faulting and that clay diapirism complicated the structure. Recent interpretations involve movement along thrusts above which the anticlines associated with mud volcanism developed (Kazantsev and Bekher, 1988).

Our aim is to bring some tectonic constraints to this debate and to understand better the tectonic evolution of this subsiding segment of a mountain belt. We carried out detailed tectonic analyses at 22 sites on the Kertch and Taman peninsulas (Fig. 3). We collected nearly 600 fault slip measurements and nearly 100 measurements of other brittle structures (joints, tension gashes and veins, stylolites, etc.). Bedding attitudes and fold axes were also measured at all sites. We used all these measurements to determine paleostress tensors and, consequently, the tectonic regimes which affected the late Cenozoic rocks of the Kertch–Taman peninsu-

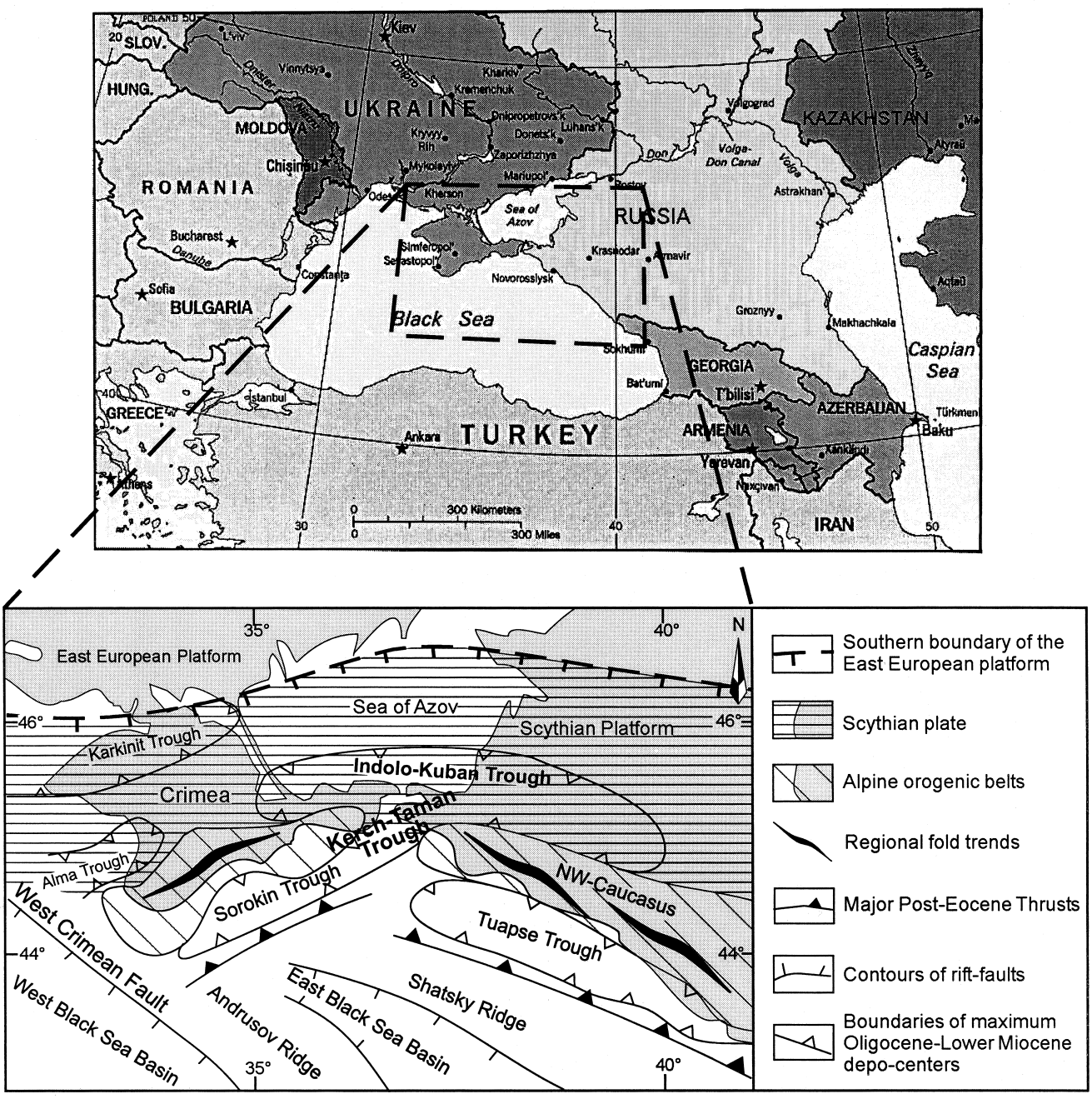

Fig. 1. Location of the studied area, from Tugolesov et al. (1985), Finetti et al. (1988) and Shreider et al. (1997).

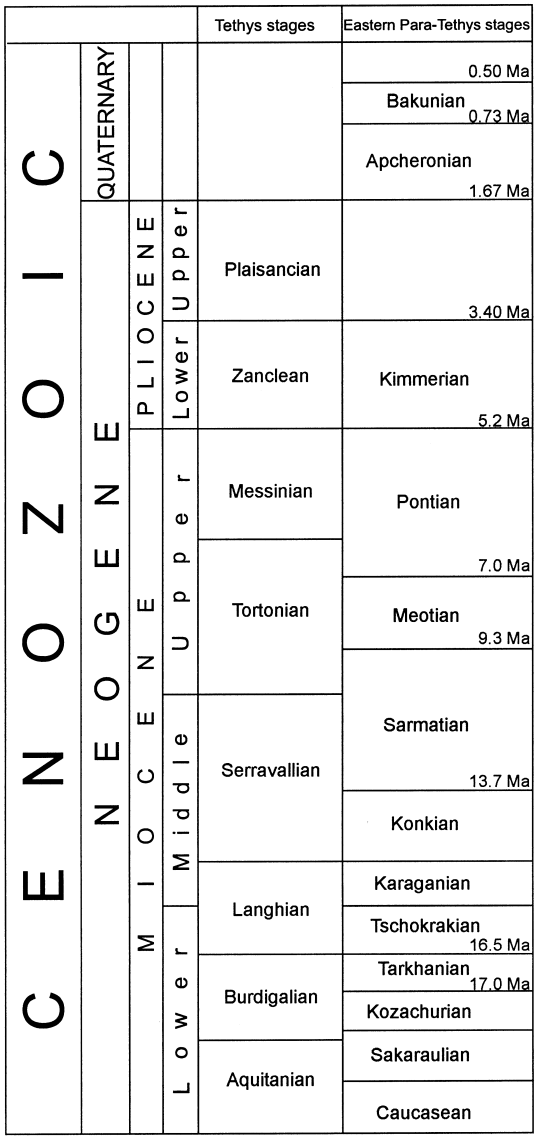

Fig. 2. Correlation of Eastern Para-Tethys stratigraphic column with Tethys stratigraphy in Neogene–Quaternary times, with absolute ages from Chumakov (1993).

las. We paid particular attention to the correlation between these tectonic regimes and the development of major structures, especially the regional folds observed throughout the whole Kertch–Taman Trough area.

2. The Kertch–Taman peninsulas

The Kertch–Taman area is a type location for studying the stratigraphy of the Neogene–Quaternary in the eastern Para-Tethys domain. Because correlation with Mediterranean stratigraphy is still a matter of debate (for example, the Pontian is the lower-most stage of Pliocene according to Ezmailov, 1996, whereas it is the latest stage of Miocene according to Nevesskaya et al., 1984), it remains necessary to use the Eastern Para-Tethys stratigraphic reference frame (see Fig. 2 for approximate ages and comparison with the Tethys domain).

At the regional scale, deep rapidly subsiding troughs began to develop during the Oligocene: the Karkinit Trough, Alma Trough, Sorokin Trough, Tuapse Trough, and the Kertch–Taman peninsulas correspond to parts of the Indolo-Kuban Trough and Kertch–Taman Trough (Tugolesov et al., 1985, Fig. 1). Trough axes are shown along the depo-centers of the Oligocene–Early Miocene Maykopian group. According to such a reconstruction, the axis of the Indolo-Kuban trough trends nearly E–W between 35°E and 38°E. In more detail, it is located in the northern Kertch peninsula west of the Kertch strait, and in the central Taman peninsula east of it (Fig. 3). Using the same approach based on sediment thickness, the axis of the Kertch–Taman trough appears to trend nearly WSW–ENE from the NE termination of the Sorokin trough (on Fig. 1) to the southern part of the Taman peninsula (Fig. 3).

The Oligocene–Lower Miocene formations of the Maykopian group crop out within ENE–WSW-trending folds in the Parpach Ridge area of the south-western Kertch peninsula (Fig. 3). Elsewhere in the study area, Maykopian formations are buried beneath younger sediments (from Tarkhanian to Quaternary). The Parpach Ridge (Fig. 3) corresponds to the eastern extension of the Crimean mountains that plunge towards the Kertch peninsula (Grigor'yants et al., 1981).

An interesting feature of the Kertch–Taman peninsulas is the widespread folding of the Neogene sedimentary complex, as compared with the adjacent segments of the Crimea–Caucasus belt. The geological map of Taman region at 1/220 000 scale (Ezmailov, 1996; Fig. 4) illustrates this general folding. The cross-section that we have established across the Zelenskiy anticline, from site 126 to site 127 (Fig. 5, located in Fig. 4) shows that folds may be relatively close with interlimb angle less than 70°. The folds are commonly asymmetrical, such as the Zelenskyi anticline (Fig. 5).

Equally characteristic of the Kertch–Taman peninsulas is the occurrence of numerous mud volcanoes and the spectacular diapirism of the Maykopian clays cutting through the overlying sediments. A close spatial and temporal link exists between the development of these features. The diapirism commonly occurs near the top of anticlines and may produce their typical noncylindrical shapes; most mud volcanoes are located near anticline hinges. As an example, Fig. 4 illustrates the relationships between these features. The ejecta from mud volcanoes are located at the top of anticlines and are dated as Middle and Late Pliocene–Quaternary (following Ezmailov, 1996). All

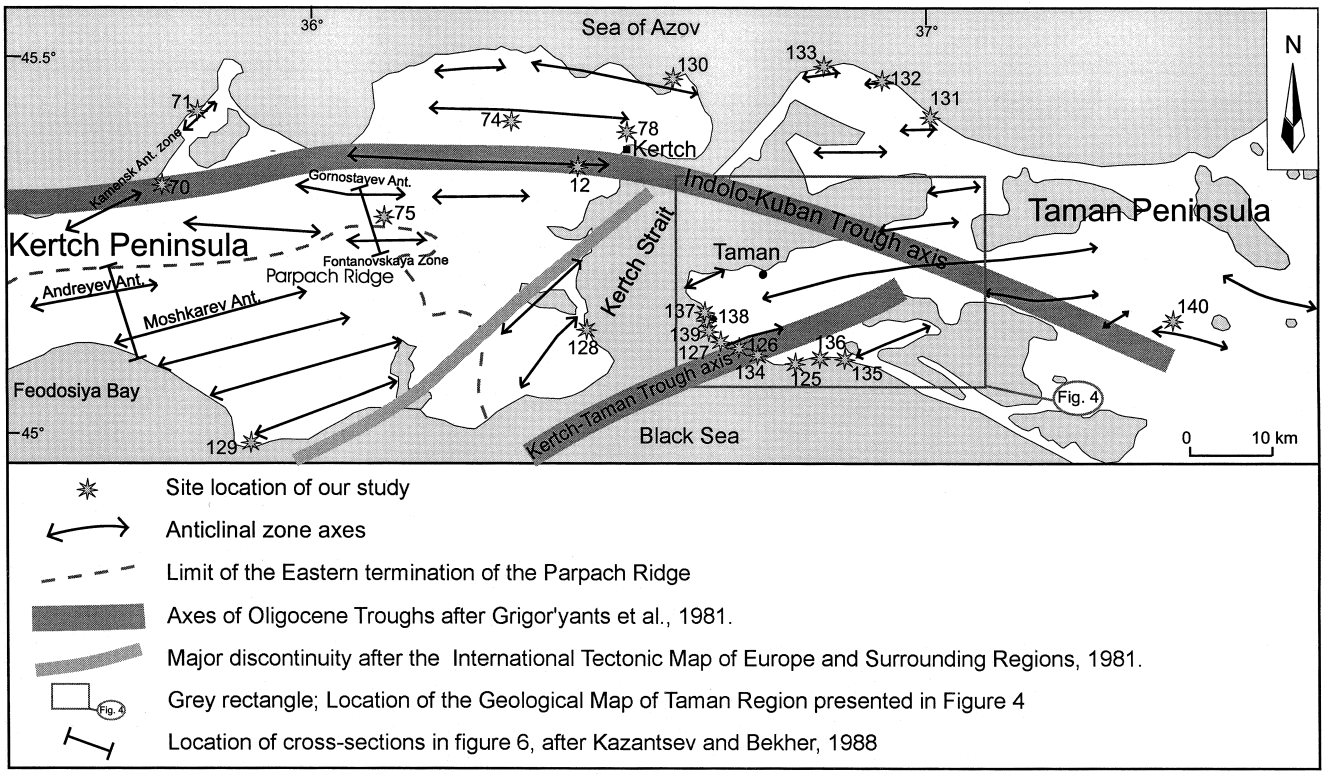

Fig. 3. Structural scheme of the Kertch–Taman peninsulas showing the distribution of fold axes and the Indolo-Kuban trough and Kertch–Taman trough axes (location of Figs. 4 and 6), compiled from Grigor'yants et al. (1981), from the geological map of the region between Caucasus and Crimea Mountains (1956) and from the International Tectonic Map of Europe and Surrounding Regions (Bogdanov and Khain, 1981).

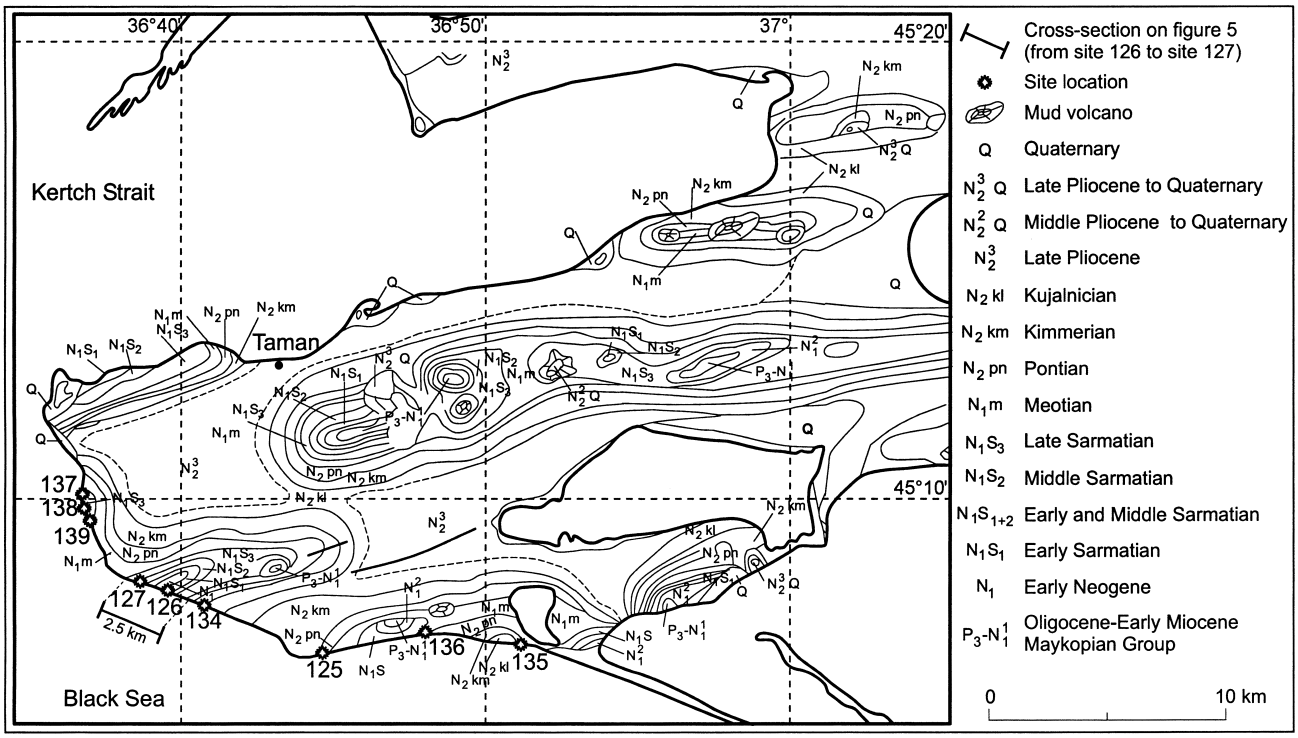

Fig. 4. Geological map of the Taman region, southern part of the Taman Peninsula (for location, see Fig. 3) showing typical structures of the studied area: non-cylindrical folding affecting all outcropping rocks, which range in age from the Oligocene to the Middle Pliocene, and mud volcano development at the hinges of anticlines, after Ezmailov (1996). The location of cross-section of Fig. 5 is shown.

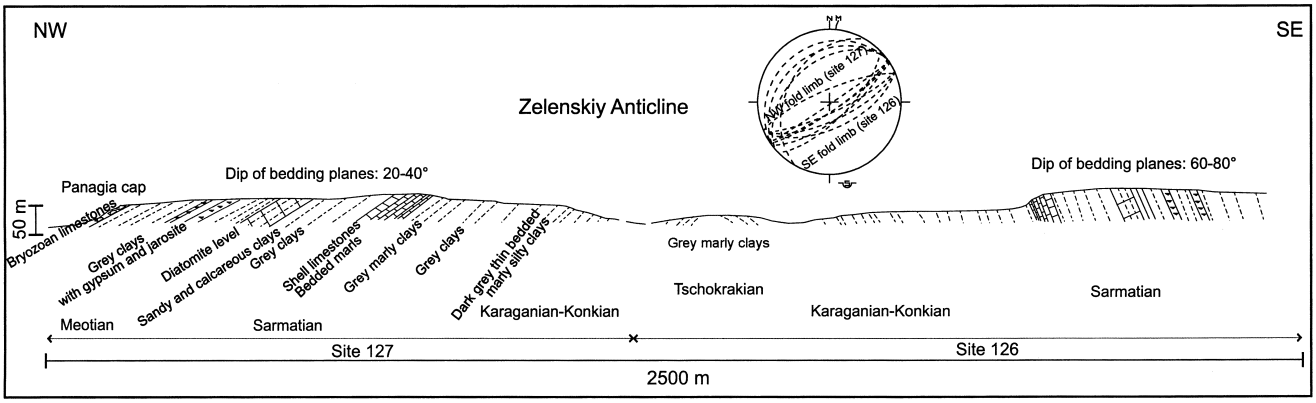

Fig. 5. Cross-section from site 126 to site 127 across the close ENE–WSW Zelenskiy Anticline (location on Fig. 4) with stereoplot of bedding plane measurements along the cross-section (note the vertical exaggeration of the cross-section).

the rocks cropping out in this fold area, which range in age from the Oligocene–Early Miocene (Maykopian Group) to the Early–Middle Pliocene, are involved in the folding except these ejecta. Furthermore, no significant tectonic unconformity was observed within these strata along the fold limbs, which strongly suggests that most of the folding post-dates the Middle Pliocene time.

Three main trends of major fold axes exist: E–W, ENE–WSW and NE–SW (Fig. 3). The E–W-trending fold axes clearly dominate to the north of both these peninsulas, along the coast of the Azov Sea. The ENE–WSW-trending fold axes are not only present in the south-western Kertch peninsula (Parpach Ridge area) but also in the south-western Taman peninsula. The NE–SW-trending fold axes are present in the south-eastern Kertch peninsula (in the vicinity of site 128) and in the Kamentsk anticline zone (in the vicinity of sites 70 and 71). WNW–ESE-trending folds are scarce, and limited to the easternmost Taman peninsula (in the vicinity of site 140, Fig. 3).

Based on interpretation of seismic cross-sections (Fig. 6), Kazantsev and Bekher (1988) assumed that the asymmetrical anticlines, and consequently the mud volcanoes, formed at ramp fronts resulting from the activation of thrusts. This structural interpretation is summarised on Fig. 6, with two typical cross-sections in the Kertch peninsula, located on Fig. 3 (Gornostayev and Fontanovskaya areas and Andreyev and Moshkarev areas, Fig. 6). Drilling in the Kertch peninsula revealed north-vergent thrusting at a depth of about 3.5 km (Fig. 6, Kazantsev and Bekher, 1988). The diapirism of clay material and associated mud volcanism is related to activation of these thrusts under a compressional regime from Late Pliocene. The present-day occurrence of mud volcanism suggests that the compressional regime is still active. Offshore seismic profiling, south of the Kertch–Taman peninsulas, also provides significant information to reconstruct the fold-and-thrust structure. These data highlighted the presence of large south-vergent thrusts involving strata as young as Quaternary (Finetti et al., 1988).

3. Paleostress tensor determination and brittle tectonic evolution

Inversion of fault slip data to reconstruct the stress tensor was carried out with methods described elsewhere in detail (Angelier, 1975, 1984, 1989, 1990). Fig. 7 summarises some important aspects of our techniques. The quality of the stress tensor determinations is variable, depending not only on the misfits and the number of data used for each determination, but also on the geological context and complementary observations. The amount of data, the average misfits and the overall quality of the determination are listed in Table 1. Determinations with limited numerical significance (especially where data are scarce or of low quality, see Table 1) were recorded provided that complementary data and observations support them. Because fault-slip data sets are often inhomogeneous and commonly reveal polyphase brittle tectonism, separation into homogeneous subsets, which correspond to different stress states and possibly to distinct tectonic events, must be carried out. This must be based on both the geological (e.g. successive slips and cross-cutting relationships, or stratigraphic control) and mechanical evidence. The latter is illustrated on Fig. 7(b) by the separation into a subset of strike-slip faults (consistent with NE–SW compression) and a subset of normal faults (consistent with NE–SW extension) within the inhomogeneous set collected at site 139 (see Fig. 3 for site location). We established the chronology of brittle events at both local and regional scales by considering a variety of criteria, including the stratigraphic ages of affected rocks, the successive striae observed on fault surfaces (Fig. 7c illustrates the

succession of two reverse slips with different orientations on a single family of faults at site 12), and the determination of post-folding or pre-folding stress states. The last is based on the assumption that one of the three principal stress axes is commonly found to be vertical or nearly vertical where no tilting has occurred during or after the brittle event. This is illustrated on Fig. 7(d) in the case of a set of present-day oblique-slip normal faults, which corresponds to a set of dip-slip normal faults predating folding, found at site 139.

Based on mechanical similarity, and controlled by the geological criteria mentioned above, the paleostress tensors computed at the local scale are grouped in order to reconstruct paleostress fields. The main regional trends are thus reconstituted for the successive tectonic regimes. This method, based on local paleostress tensor reconstruction, allows determination of tectonic evolution at the regional scale (e.g. Mattauer and Mercier, 1980; Barrier and Angelier, 1986; Letouzey, 1986; Bergerat, 1987; Mercier et al., 1987). All the quantitative results in the Kertch–Taman peninsulas are listed in Table 1 and the sites are located on Fig. 3.

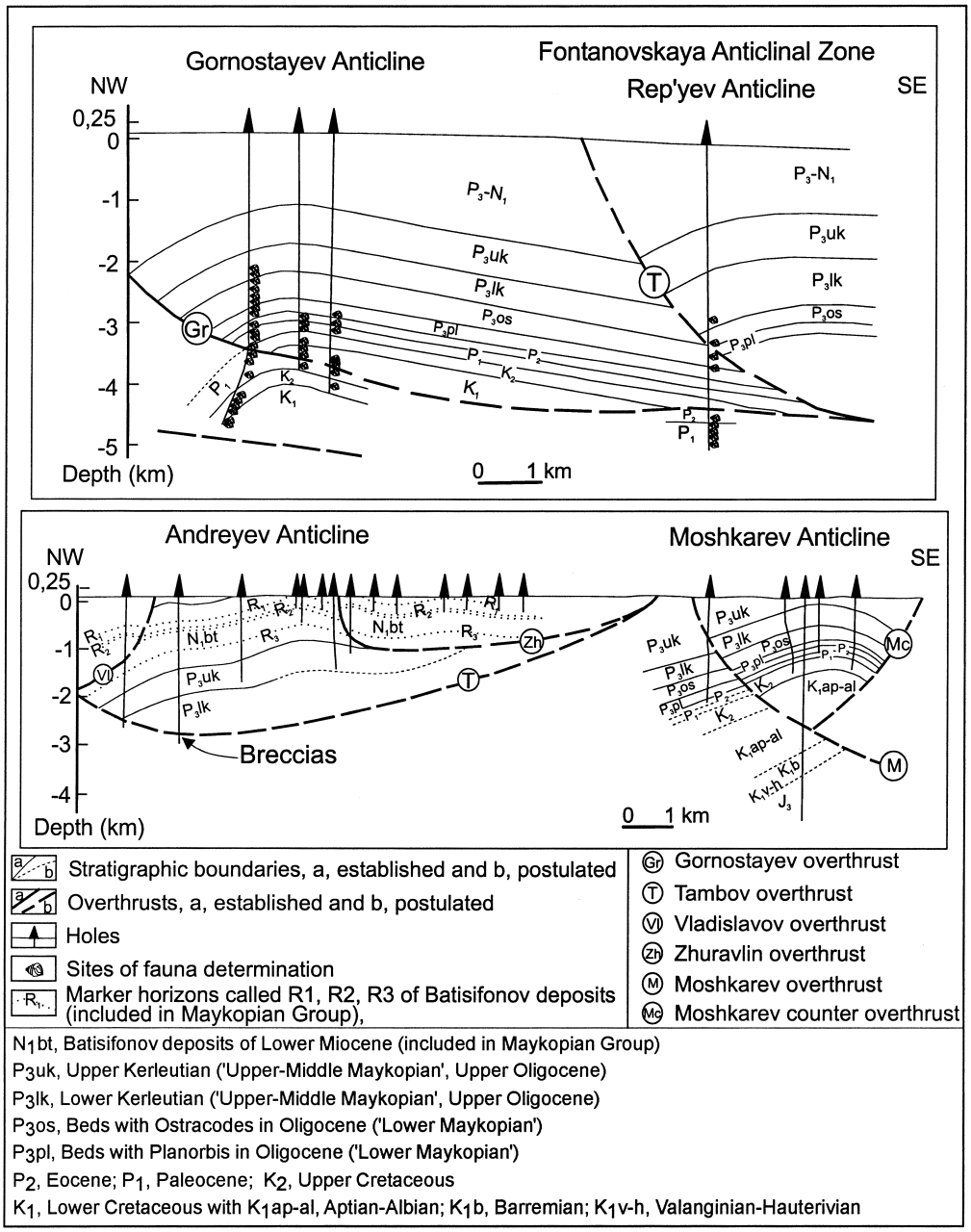

Fig. 6. Seismic profile interpretation in Kertch Peninsula across anticline structures (for location, see Fig. 3), showing close genetic relationships between thrust ramps and anticlines, from Kazantsev and Bekher (1988).

To summarise, these results revealed two main paleostress fields that affected the rocks of the Kertch–Taman peninsulas, as described below.

3.1. Extensional event

Fig. 8 illustrates an extensional event that we could reliably determine at only few places in the Kertch–Taman area. This event locally predates the tilting related to folding (e.g. Fig. 7d). Four stress tensors (at sites 131, 137, 138, 139, see Fig. 8) have been backrotated according to the attitude of bedding planes and assuming that folds are cylindrical, with nearly horizontal axes. (We have not taken into account rotation of bedding planes which could have occurred around vertical axis.)

The directions of extension are scattered. As Table 1 and Fig. 8 show, they vary from NNW–SSE (site 137) to E–W (site 131). Because corresponding sites are few, the average trend of extension, NE–SW (as for sites 138 and 139) has little significance. This scattering of directions of extension could be explained by the fact that we have considered that folds are cylindrical in order to backrotate the stress tensors; this is not the case in the Kertch–Taman peninsulas, where most folds are noncylindrical.

This extensional paleostress affects Sarmatian rocks (site 137 and 138), Meotian rocks (site 139) and the Pliocene rocks (Kimmerian or Kuyalnician) at site 131. That we never found stratigraphic evidence for an earlier extension is not sufficient to claim that the regional paleostress described on Fig. 8 is monophase, at Pliocene times. We conclude that the existence of Late Cenozoic extension in the Kertch–Taman area is beyond doubt, although both its distribution and uniqueness deserve further investigation.

3.2. Compressional event(s)

Most stress tensors are compatible with the orientation of the Plio-Quaternary folding deformation (Fig. 9). In other words, the trend of compressional

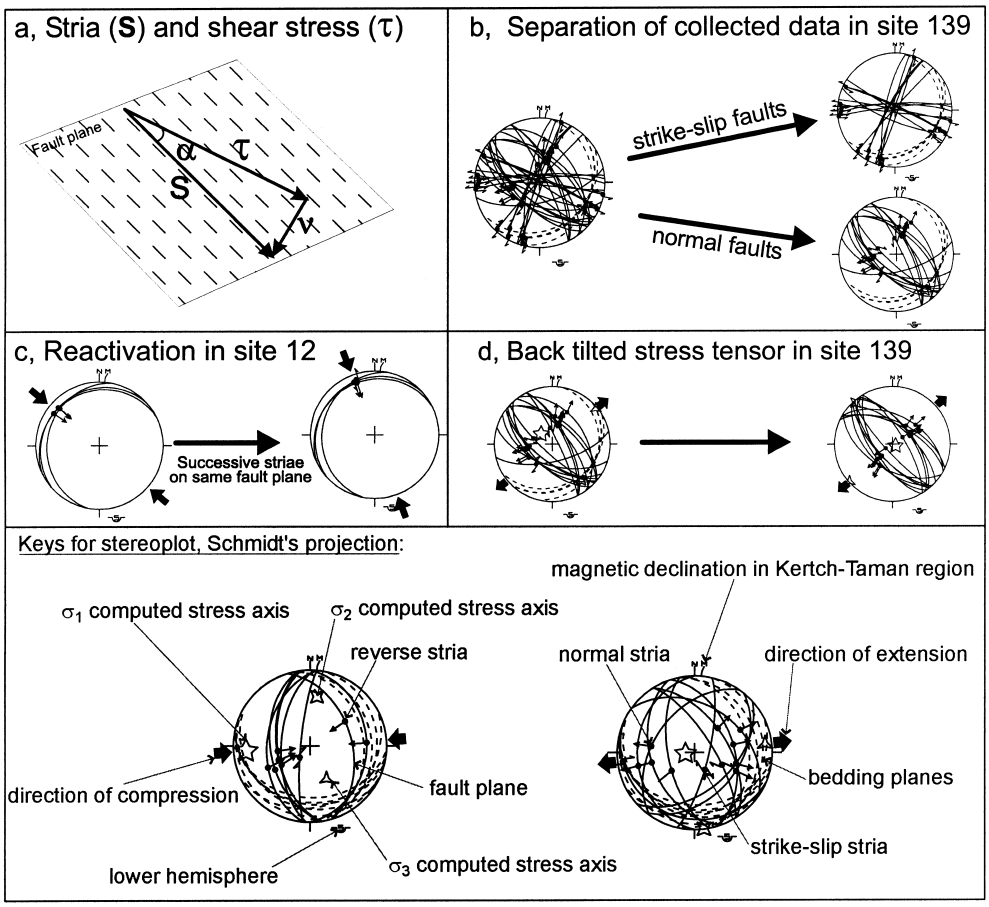

Fig. 7. (a) Illustration of the inversion method based on the Wallace and Bott principles (respectively, Wallace, 1951 and Bott, 1959): 'the shear stress τ is parallel to the stria s'; the INVD method (Angelier, 1990) minimizes the difference v between the real striae s and the calculated shear stress τ and also, the angle α. (b–d) Examples of polyphase tectonism. (b) Fault population collected in site 139 near Taman. The whole set is divided into two subsets, consistent with different stress regimes. (c) Reactivated fault as shown by superposed sets of striae; site 12, near Kertch. (d) Back-tilted stress tensor site 139 near Taman.

Table 1
Paleostress results at sites studied in Kertch–Taman area. no., reference number of the site. Stress regimes: S, strike-slip faulting; R, reverse faulting; N, normal faulting. n, number of fault slip data. Trends and plunges of stress axes in degrees (with * for back-tilted stress tensors). Methods (INVD and R4DT) referred to in Angelier (1990). Φ, ratio of stress magnitude differences, $\Phi=(\sigma_2-\sigma_3)/(\sigma_1-\sigma_3)$. α, average angle between observed slip and computed shear, in degrees (acceptable with $\alpha < 22.5°$). RUP, criterion of quality for the 'INVD' method, ranging from 0% (calculated shear stress parallel to actual striae with the same sense and maximum shear stress) to 200% (calculated shear stress maximum, parallel to actual striae but opposite in sense), acceptable results with RUP < 75%. Q is quality from 1 (poor result) to 3 (high quality)

Localities	Lat./Long. In degrees	Age of formation	no.	Stress regime	n	σ_1 trend	σ_1 plunge	σ_2 trend	σ_2 plunge	σ_3 trend	σ_3 plunge	Meth.	Φ	α	% RUP	Q
	45.32/36.34	Meotian	12	R	19	124	08	033	02	290	82	INVD	0.5	11	39	3
			12	R	16	160	11	251	05	004	78	INVD	0.5	08	30	3
	45.37/36.26	Meotian	74	R	10	212	06	303	10	093	79	INVD	0.4	10	38	3
	45.40/36.42	Meotian	78	R	4	354	12	084	02	182	77	INVD	0.6	04	9	1
Kertch	45.15/36.42	Meotian	128	R	17	319	02	049	01	182	88	INVD	0.6	04	11	3
	45.00/35.85	Maykopian	129	R	Reverse faults associated with folding in N–S compressional event											
	45.42/36.55	Tarkh. to Sarmatian	130	R	36	132	08	042	01	304	82	INVD	0.4	10	31	3
			130		N150 shortening trend (σ_1') deduced from fold axes measurements											
			130		N110 shortening trend (σ_1') deduced from fold axes measurements											
	45.13/36.66	Sarmatian–	126–127	R	Some reverse faults developed in a N120 compressional trend before tilting											
		Meotian	126–127	R	10	151	02	241	06	043	83	INVD	0.3	8	23	3
			126–127	S	Some strike-slip faults associated in NW–SE compression											
			126–127	R	7	161	07	254	18	051	71	INVD	0.4	11	35	1
			126–127	N	6	196	77	063	09	331	09	INVD	0.4	06	19	1
	45.37/37.08	Pliocene	131	R	6	265	17	008	35	154	50	INVD	0.2	05	19	2
			131	R	5	012	01	282	09	110	81	INVD	0.6	03	12	1
			131	N	12	264	81	173	00	083	09	INVD	0.4	14	30	2
			*	N	12	135	79	351	09	260	06	INVD	0.4	11	26	2
			131	S	6	169	25	005	64	262	06	INVD	0.2	06	27	2
	45.11/36.85	Pontian	135	S	Some strike-slip faults associated in a N115 compressional event											
Taman	45.17/36.60	Sarmatian	137	R	10	009	12	101	08	225	75	INVD	0.5	08	22	3
			137	N	23	234	77	071	13	340	04	INVD	0.3	07	22	3
			*	N	23	325	80	069	03	159	10	INVD	0.3	07	22	3
	45.16/36.60	Sarmatian	138	R	15	111	12	020	04	274	78	INVD	0.7	08	17	3
					Associated folding											
			138	N	25	283	57	102	33	192	00	INVD	0.3	17	37	3
			*	N	25	286	73	113	16	022	02	INVD	0.3	16	36	3
	45.15/36.62	Meotian	139	R	7	322	01	52	14	228	76	INVD	0.4	04	10	3
			*	R	7	319	12	050	03	152	77	INVD	0.4	05	10	3
			139	N	15	313	69	142	21	051	03	INVD	0.3	05	25	3
			*	N	14	119	85	319	04	229	02	INVD	0.4	05	25	3
	45.08/37.50	Pontian–	140	N	8	165	77	288	07	019	11	INVD	0.3	08	29	2
		Kimmerian			Associated tension gashes											

stress was often, albeit not systematically, approximately perpendicular to the axes of folds. In addition, some evidence of extension at anticline hinges was detected, and these structures were carefully distinguished from the evidence of genuine extension shown on Fig. 8. Such a local extension is geometrically related to the fold shape, and generates normal faulting at the hinges, as for site 140 and site 126 on Fig. 9.

As Table 1 and Fig. 9 show, the directions of compression are distributed around two main trends, nearly N–S and NW–SE. An E–W compression is determined at site 131, but seems to be local. Trends of major fold axes discussed before are compared to the trends of compressional stress axes (Fig. 9). There is a general tendency to perpendicularity, although oblique compression also occurs. In the northern part of the Kertch–Taman peninsulas, where the axes of anticlines trend nearly E–W, analysis of brittle structures reveals an approximately N–S-trending compression (e.g. sites 78 and 131, Fig. 9). NW–SE compressions are also present, 45° oblique to fold axes (e.g. sites 12 and 130, Fig. 9). In the southern part of the Kertch–Taman peninsulas, where the axes of anticlines trend ENE–WSW or NE–SW, our analyses often revealed an approximately NW–SE-trending compression (e.g. sites 128 and 126–127, Fig. 9). Some nearly N–S compression, 45° oblique to fold axes, is however present in this area (e.g. sites 137 and 126, Fig. 9).

To summarise, most of the detected compression is found parallel to the shortening deduced from major fold axes. As a consequence, because there are two major regional trends of fold axes, E–W and NE–SW, two main directions of shortening are inferred, approximately N–S and NW–SE. There is a rough spatial correlation between the compressional trends and the directions of shortening (Fig. 9). Each of these compressions affects in a significant way the whole of the Kertch–Taman peninsulas. This is especially the case for the NW–SE compression, recorded at three sites in the northern Kertch peninsula where shortening is N–S directed as deduced from large E–W-trending fold axes (Fig. 9).

3.3. Tectonic chronology

To determine whether the inferred compressional events correspond to a single-phase of tectonism or not, it is necessary to examine the chronological evidence (for site location, fold trends and directions of compression, see Fig. 9).

The NW–SE compression corresponds principally to reverse faulting (strike-slip faulting developed in sites 126–127 and 135 is in agreement with this compressional regime) affecting rocks dated from Tschokrakian to Meotian (site 126–127), Sarmatian (site 138), Meotian (sites 12, 128 and 139), and Tarkhanian to Sarmatian (site 130). At all these sites, the direction of

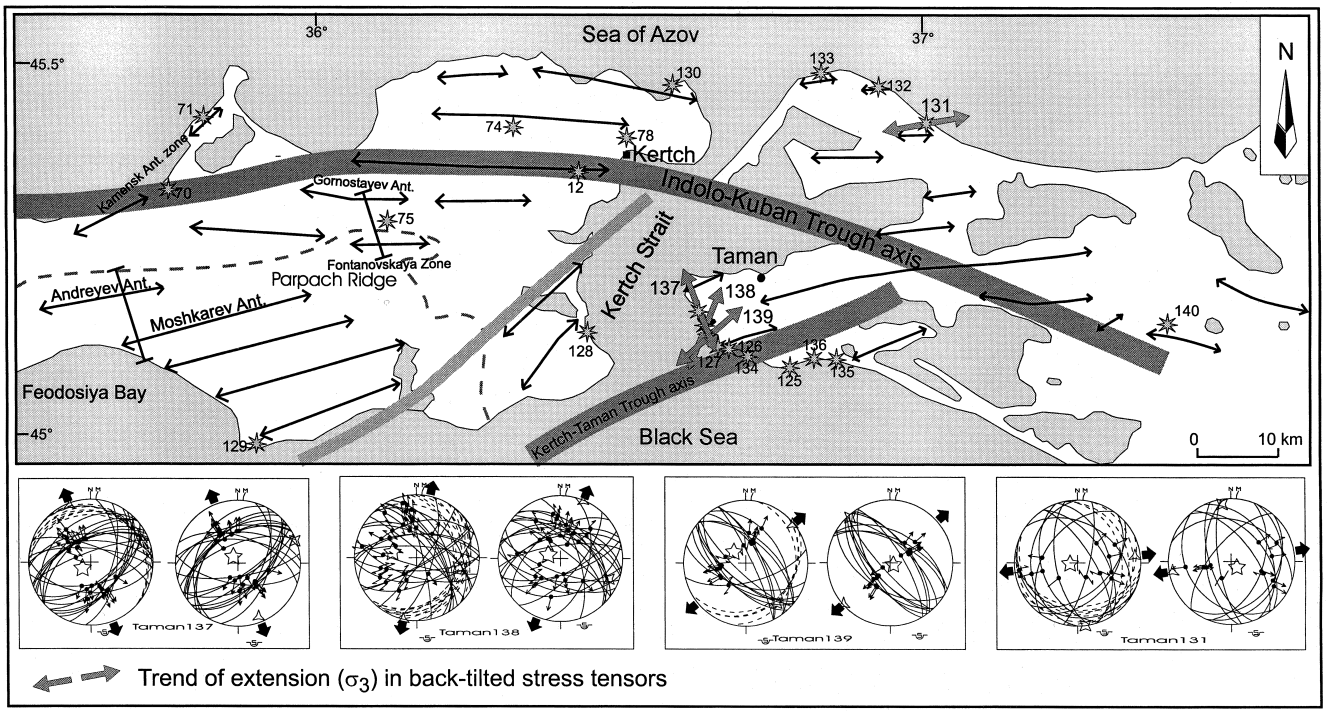

Fig. 8. Results indicating an extensional event before the folding of terranes in the Kertch–Taman area. Caption of structural map as for Fig. 3, keys for stereoplot in Fig. 7.

compression is perpendicular to the direction of folding. At site 126–127, we observed normal faults, resulting from additional extension at anticline hinges. It is interesting to note that the reverse faulting (compatible with NW–SE compression) predates folding at sites 126–127 and 139.

The N–S compression is accommodated by strike-slip and reverse faulting in rocks dated as Sarmatian (site 137), Meotian (sites 74 and 78), and Pliocene (site 131). All these sites belong to the northern domain of E–W-trending folds, so that this direction of compression is also compatible with the folding. Considering that the anticline at site 140 belongs to the same group of E–W folds, extension occurs locally at fold hinges, as for the other group of folds.

At sites 12 and 126–127, we could not only determine two directions of compression related to subsets of reverse faults, but also establish their relative chronology based on the cross-cutting of successive striations on fault surfaces. The oldest compression was trending NW–SE, and NE–SW-trending dip-slip reverse faults developed as conjugate systems (see stereoplots of site 12 on Figs. 9 and 7c). In addition, in site 126–127, some reverse faults developed before folding in the first NW–SE directed compressional event. Later, after the folding, these fault surfaces were reactivated as oblique-slip reverse faults under a nearly NNW–SSE compression (see stereoplots of site 126–127 on Fig. 9). At site 130 near Kertch, we could determine a single stress tensor indicating NW–SE compression, but we also observed two sets of disrupted minor fold axes associated with reverse faulting, compatible with NW–ESE and nearly N–S directions of compression, respectively. These observations suggest that two successive compressional events, NW–SE first and nearly N–S second, have controlled the folding deformation in the Kertch–Taman peninsulas.

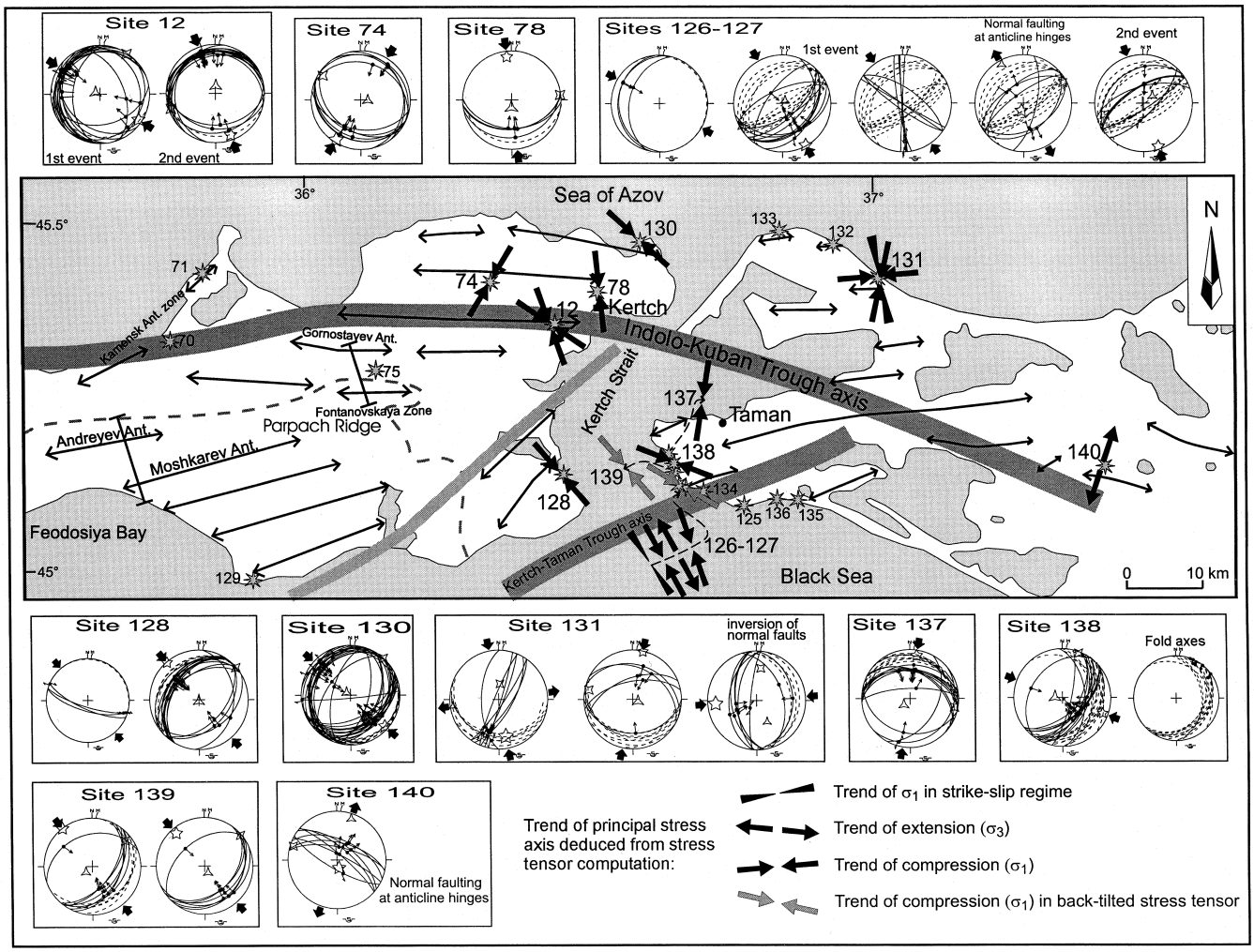

Fig. 9. Plio-Quaternary compressional event in agreement with the folding deformation and related stress tensor stereoplots. Caption of structural map as for Fig. 3, keys for stereoplot in Fig. 7.

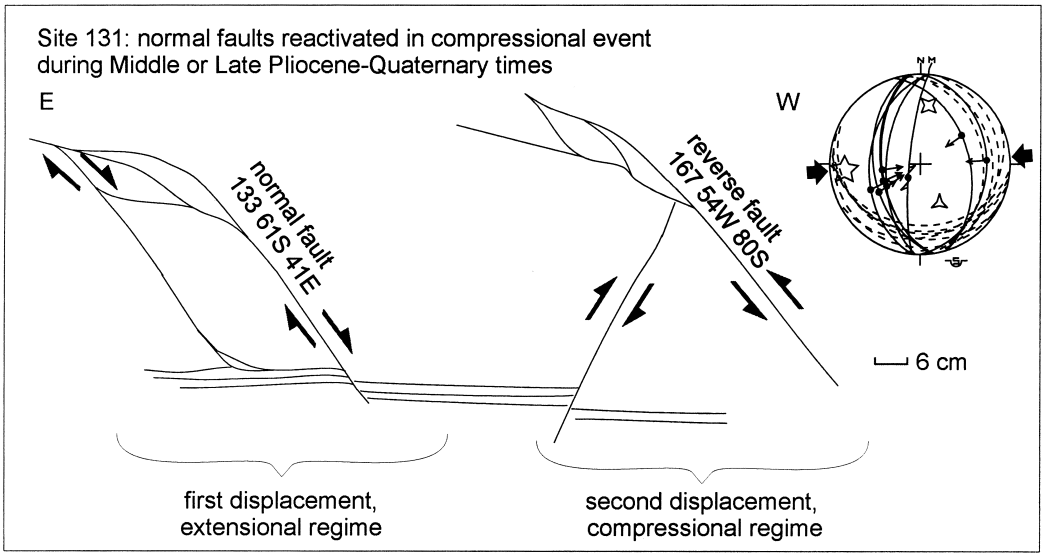

Fig. 10. Local inversion of normal fault system in E–W directed compression (in Pliocene sandstone formation, site 131). Explanations for fault measurements: 133 61S 41E means strike azimuth, dip, dip direction, pitch and pitch direction, respectively. Keys for stereoplot in Fig. 7.

In the Pliocene formations at site 131 a particular E–W compression induced reactivating of earlier minor normal faults as reverse faults, resulting locally in structural inversion (Figs. 9 and 10). This compression is in agreement with the tilting of bedding. We interpret this E–W compression as related to secondary along-strike contraction within the E–W-trending major fold system. The presence of transverse vertical faults could confine the development of folds, creating a local E–W contraction; such faults exist in the Gornostayev anticline and Rep'yev anticline areas (Alekseyev and Fontanov faults as shown on Fig. 11), but we do not know if they exist in the vicinity of the E–W anticline near site 131. The N–S-trending major compression also affected this site (Fig. 9). Whatever the explanation, this site 131 provides additional evidence that regional extension predated the Late Pliocene–Quaternary compressional tectonism (for both the folds and the reverse faults) in the Kertch–Taman region.

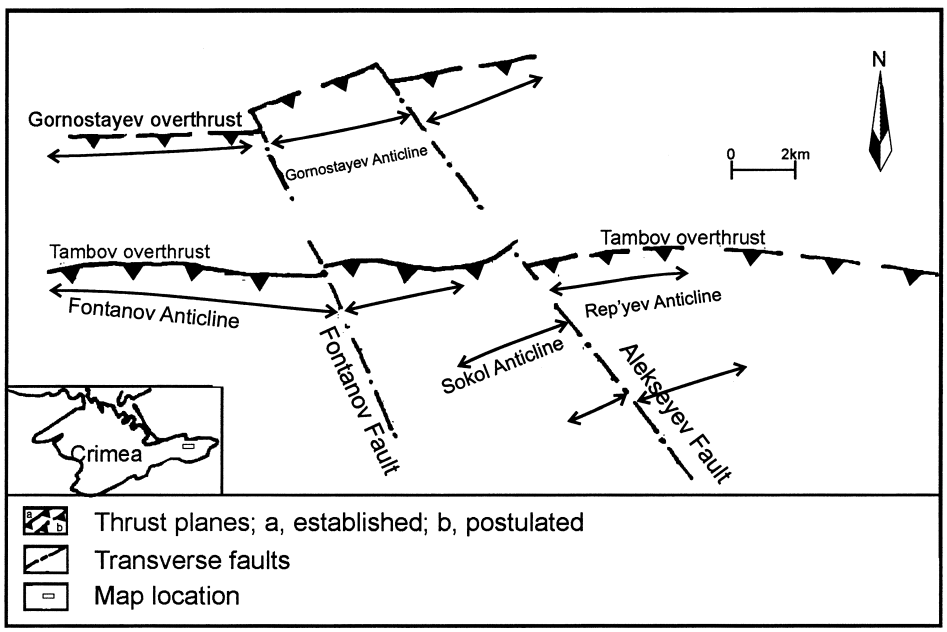

Fig. 11. Example of vertical faults trending transverse to the fold axes, in Gornostayev anticline and Rep'yev anticline areas, from Kazantsev and Bekher (1988). Such faults (if they exist in the vicinity of site 131) could be an explanation to E–W contraction along the E–W-trending fold axis by confining the fold development.

Because the extension also occurred before the folding event at sites 131, 137, 138 and 139, and the compressions that we determined are correlated with folding, the relative chronology between extension and compression is clearly established.

The complex pattern of fold trends and directions of compressions presented on Fig. 9 could have resulted from intricate structural accommodation phenomena within the frame of a single major event of NNW–SSE contraction across the belt, during the Late Cenozoic. However, all observations presented above suggest that the NW–SE compression significantly predated the N–S compression. According to this interpretation, the N–S compression, perpendicular to the late Cenozoic structural grain of the belt in the Kertch–Taman region, corresponds to the most recent contractional event, whereas the NW–SE compression, nearly perpendicular to the major trend of the Crimea belt, prevailed during an earlier stage of the Late Cenozoic (probably Late Pliocene).

4. Relationships with structural evolution of the NW-Caucasus–Crimea belt

4.1. Basin development and extension

We conclude that the extensional regime that affected the Kertch–Taman region before folding, was related to the development of the Kertch–Taman and Indolo-Kuban troughs, which began at Oligocene times. Based on stratigraphic studies, Nikishin et al. (1998) identified high rates of subsidence in these troughs during several periods in Neogene times: Tschokrakian–Karaganian, 16.5–15 Ma; Middle and Late Sarmatian, 12.4–9.7 Ma; Pontian, 7–5 Ma; Kuyalnician, 3.7–1.8 Ma. The normal faulting identified at site 131 probably results from the last period. The relationship between high subsidence rates and normal faulting may result from deep-seated extension in a typical extensional basin or from extensional processes accompanying the development of a flexural basin.

Nikishin et al. (1998) argue that no widespread normal faulting was associated with the subsidence phases and propose a flexural origin for the trough development. Most authors agree that the closure of the Tethys ocean between the Arabian Plate and the East European Craton in the Late Eocene times, induced a collisional stage in the whole Caucasian region (Khain, 1950; Khain and Shardanov, 1957; Milanovsky and Khain, 1963; Muratov et al., 1984; Leonov, 1985; Maisadze, 1994; Robinson et al., 1996; Nikishin et al., 1998, in press) and the Great Caucasus fold-and-thrust belt development, from Crimea to the Caspian Sea (Zonenshain et al., 1990; Milanovsky, 1991, 1996). According to Bolotov and Nikishin (1995) and Bolotov (1996), the regional subsidence and the Oligocene flexural trough formation were related to the retreat or the detachment of a major Tethys slab under the Caucasus region. If these troughs are flexural in type, the normal faulting in the Kertch–Taman peninsulas can reflect the elongation of the upper lithosphere as a result of bending and downwarping during the periods of rapid subsidence.

Nikishin et al. (in press) acknowledge, however, that the mechanisms of this rapid subsidence, which affected the whole Black Sea domain (Spadini et al., 1997; Korotaev, 1998), are poorly understood. Although the development of flexural troughs is beyond doubt, the formation of the Kertch–Taman trough itself seems difficult to explain in terms of flexure because of its singular location across the belt. In contrast, the Indolo-Kuban trough trends parallel to the Crimea–Caucasus belt, and resembles a typical foreland basin. During the Kertch–Taman trough development, the deep-seated discontinuity (Bogdanov and Khain, 1981) mapped across the south-eastern Kertch peninsula may be evidence for a major crustal normal fault (Fig. 3). In addition, high concentrations of deep crustal or mantle elements are recorded in the Kertch–Taman rocks (Al'bov, 1974), suggesting again that deep-seated faults are involved. The existence of such deep structures could be consistent with deep-seated extension to explain the presence of the Kertch–Taman trough across the Crimea–Caucasus fold-and-thrust belt but does not suffice to exclude flexural trough development as the major driving mechanism.

In any case, our determinations of extensional stress tensors in the Kertch–Taman area confirm that deviatoric stresses were associated with deep trough development. More general tectonic analyses, carried on in the Crimean and NW-Caucasus belts, have already suggested that extensional stress tensors were associated with Oligocene–Neogene trough development (as the Tuapse and Sorokin troughs, located on Fig. 1; Saintot et al., 1995, 1996, 1998, 1999).

4.2. Compressional events

The present-day structures of Taman and Kertch peninsulas result from a major contraction of the thick sedimentary sequences of the previously formed Kertch–Taman trough. This tectonic event is a NW–SE to nearly N–S compression, probably related to detachment folding (as shown by subsurface studies, Fig. 6; Kazantsev and Bekher, 1988), in which all the Late Cenozoic rocks including the Quaternary are involved. This late age of compression is consistent with the recent activity of mud volcanoes developing in the core of associated anticlines. In more detail, our tectonic analyses suggest that the NW–SE compression

predates the N–S one, although they both correspond to a tectonic regime of contraction.

The recent compressional tectonism that we have discussed in this paper results from the NNW–SSE convergence between the Eastern Black Sea System (i.e. the Eastern Black Sea Basin and the Shatsky Ridge, Fig. 1) and the Scythian plate southern margin. We propose that the deviation in the trends of major structural grain throughout the Kertch–Taman peninsulas results mainly from a kind of indentation phenomenon (the Black Sea side, to the south, representing the indentor). The Kertch–Taman trough and the Indolo–Kuban trough developed between earlier established major structural grains—the NW–SE-trending Caucasus belt and the ENE–WSW Crimean mountains. It follows therefore that subsequent compressive deformation is extremely sensitive to variations in the direction of convergence. The complexity of the compressional pattern in the Kertch–Taman region (Fig. 9) probably results from related structural accommodation.

Because the formations cropping out in the Kertch–Taman peninsulas are from Neogene to Quaternary in age, the tectonic history that we determined in this area is tightly constrained in age and can be compared with the latest tectonic history of the surrounding regions, where most exposed formations are older. Such a comparison suggests that some of the stress regimes that we could identify in older formations of the Crimean Mountains and the fold-and-thrust belt of NW-Caucasus belong to the latest compressional event, based on similarities between orientations of principal axes (Angelier et al., 1994; Saintot et al., 1995, 1996, 1998). Furthermore, in the eastern Crimean chain and neighbouring areas, the latest deformation identified by remote sensing analysis is in good agreement with the compressional stress state identified in the field (Saintot et al., 1999). We conclude that the N–S to NW–SE compression, far from being restricted to the Kertch–Taman area, affects the whole northern margin of the east Black Sea basin. Our results fit well with the fan-shape present-day stress field independently reconstructed by Goushtchenko et al. (1993) based on the inversion of focal mechanisms of earthquakes. The general NNW–SSE orientation of the present-day compressional trajectories in the Kertch–Taman region (Fig. 12) corresponds to the averaged trend of the Late Cenozoic compression (Fig. 9).

The underlying structure could also be involved to explain the difference in the fold axis trends, as suggested by Grigor'yants et al. (1981). The ENE–WSW trend of fold axes in the Parpach Ridge may simply reflect the presence of similarly trending buried structures within the Crimean chain. In the northern Kertch–Taman peninsulas, the E–W trends of fold axes are the same trends as for the Indolo-Kuban trough axis. In the southern Taman peninsula, the fold axes trend ENE–WSW, parallel to the pre-existing Kertch–Taman trough (Fig. 3). The major NE–SW-trending crustal discontinuity mapped across the south-eastern Kertch peninsula (Bogdanov and Khain, 1981) could be a feature controlling the NE–SW trend of fold axes in the vicinity of site 128 (Fig. 3). The pre-existing trend of troughs (Indolo-Kuban and Kertch–Taman) could have controlled the thrusting and folding deformation at surface: the trend of contraction could have been modified, becoming perpendicular to the margin of the troughs, and controlling the local attitudes of the new structures (thrusts and folds). In this model, a single general trend of contraction would have prevailed and deviations would have occurred mainly because of the pre-existing troughs. Another explanation for such deviations is the occurrence of thrust sheets (Fig. 6). Because thrusting occurs at different depths in the thick sedimentary sequences, the directions of compression in the uppermost units and the direction of tectonic transport may differ significantly. Thrust sheet development (Fig. 6) may thus

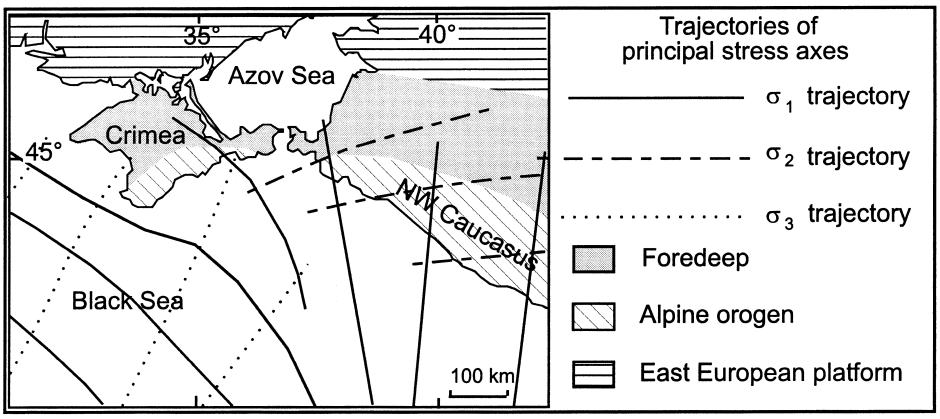

Fig. 12. Present-day stress field reconstructed by focal mechanism inversion (from Goushtchenko et al., 1993).

play a role in the scatter of the directions of compression in a continuous single-phase tectonism.

Our paleostress analyses may be used to discuss another hypothesis explaining the spatial distribution of folding. The main thrust sheets are north-vergent according to Kazantsev and Bekher (1988). The thrust–fold front was probably propagating from south to north. Keeping in mind that the N–S compression generally followed the NW–SE compression, and considering that the compressional deformation was a consequence of the convergence of the East Black Sea basin with the Scythian plate, one may infer that, during the Late Cenozoic, the convergence was first NW–SE, and developed the structural grain of the southern Kertch–Taman peninsulas. Later, the direction of convergence may have rotated clockwise to become closer to N–S. Because northward propagation of the deformation front took place in the meantime, newly formed E–W-trending fold systems developed in the northern Kertch–Taman peninsulas, while oblique reactivation of the earlier structures prevailed to the south. This alternative interpretation has the potential to explain clearly not only the chronology of tectonic events, but also the existence of contrasting directions of compression. In contrast, a scatter of trends around a dominant direction would have been expected in the case of continuous single-phase tectonism. However, this scheme fails to account for the presence of the NE–SW-trending folds of the Kamensk Zone in the north-western Kertch peninsula (Fig. 3).

Finally, it should be noted that these two hypotheses can be combined, considering that the influence of large structures at depth and the northward-propagating deformation front may have coexisted with a clockwise change of convergence direction during the Late Cenozoic. The consequences for the structural development of the Kertch–Taman belt segment have been intensified by the particular location of this segment, at the junction between the NW–SE-trending Caucasus belt and the ENE–WSW Crimea mountains.

5. Conclusions

Paleostress analyses allow us to propose a model for the tectonic evolution of the Kertch–Taman peninsulas. The early development of major troughs, including the transverse Kertch–Taman trough, played a major role. The occurrence of normal faulting (before folding) is mainly related to these troughs, and may correspond to the periods of maximum subsidence up to Kuyalnician times. Structures in the Indolo-Kuban trough support a hypothesis of flexural basin formation with normal faults as near-surface accommodation structures during periods of high rates of subsidence. (Re-?)activation of deep-seated discontinuities could have additionally controlled the development of the Kertch–Taman trough, cross-cutting the Crimea–Caucasus fold-and-thrust belt.

In Late Pliocene–Quaternary times, the Kertch–Taman region was affected by a major compressional event, resulting in folding and thrusting within the thick terrigeneous sequences of the Late Cenozoic. Widespread clay diapirism and mud volcanism developed, in relation to thrust activation at depth and anticline development closer to the surface. This major phase of NNW–SSE contraction was inhomogeneous in time and space, for both the directions of folding and the trends of compressions. NW–SE and N–S compressions are distinguished, the N–S one being generally more recent and better represented in the northern part of the area. We infer that the particular structural development of the Kertch–Taman peninsulas results from the combined effects of (1) the presence of pre-existing major structures like the Indolo-Kuban trough, (2) the northward propagation of the deformation front of the belt, (3) a limited clockwise change of the convergence direction between the Black Sea and the Scythian Plate and, (4) the amplifying role of indentation phenomena related to the geometry of the Kertch–Taman peninsulas, lying between the differently oriented mountain belts of the NW-Caucasus and Crimea.

Acknowledgements

The authors thank the Peri-Tethys Program for supporting field work, the French M.E.S.R. and the Society 'Secours des Amis des Sciences' for providing grants for the first author, and A. Ilyin who made field trips possible.

References

Al'bov, S.V., 1974. Geochemical environment in the Kertch–Taman region and nearby areas. Doklady akademya Nauk SSSR, Earth Sciences Section 208, 222–224.

Angelier, J., 1975. Sur l'analyse de mesures recueillies dans des sites faillés: l'utilité d'une confrontation entre les méthodes dynamiques et cinématiques. Comptes Rendus Academie Science Paris série D 281, 1805–1808 Erratum: Ibid., (D), 1976, 283, p. 466.

Angelier, J., 1984. Tectonic analysis of fault slip data sets. Journal of Geophysical Research 89 (B7), 5835–5848.

Angelier, J., 1989. From orientation to magnitudes in paleostress determination using fault slip data. Journal of Structural Geology 11, 37–50.

Angelier, J., 1990. Inversion of field data in fault tectonics to obtain the regional stress. III: A new rapid direct inversion method by analytical means. Geophysical Journal International 103, 363–376.

Angelier, J., Goushtchenko, O.I., Saintot, A., Ilyin, A., Rebetsky, Y., Vassiliev, N., Yakovlev, F., Malutin, S., 1994. Relations entre champs de contraintes et déformations le long d'une chaîne com-

pressive-décrochante: Crimée et Caucase (Russie et Ukraine). Comptes Rendus Academie Sciences Paris, série II 319, 341–348.

Barrier, E., Angelier, J., 1986. Active collision in Eastern Taïwan: the coastal range. Tectonophysics 125, 39–72.

Bergerat, F., 1987. Stress fields in the European platform at the time of Africa–Eurasia collision. Tectonics 6, 99–132.

Bogdanov, A.A., Khain, V.E., 1981. International Tectonic Map of Europe and Surrounding Regions (original title: Carte tectonique internationale de l'Europe et des régions avoisinantes), 1/2 500 000, 11th sheet, Congrès géologique international, Commission de la carte géologique du Monde, sous-commission de la carte tectonique du Monde. Academy of Sciences of USSR, UNESCO, CCGM, General Direction of Geodesy and Cartography to the Minister Council of USSR.

Bolotov, S.N., 1996. Mesozoic–Cenozoic geological history of the scythian platform and quantitative characteristics of the main stages of the evolution according to computer modelling. Candidate to Science dissertation (Ph.D. thesis). Moscow State University, Moscow, 320 pp. (in Russian).

Bolotov, S.N., Nikishin, A.M., 1995. Mesozoic–Cenozoic evolution of the Crimea–Peri-Caucasus sedimentary basin. EUG 8, Strasbourg, 9–13 April 1995. Abstract supplement no. 1 to Terra Nova 7, 181.

Bott, M.H.P., 1959. The mechanics of oblique slip faulting. Geological Magazine 96, 109–117.

Chumakov, I.S., 1993. Radiometric scale for the Late Cenozoic of Para-Tethys, 12. Priroda, Russia (in Russian).

Ezmailov, Y., 1996. Geological map of the Taman region, 1/220 000. In: Popov, S.V. (Ed.), Excursion guidebook, Neogene Stratigraphy and Palaeontology of the Taman and Kerch peninsulas, Field symposium 4–14th June, 1996, IGCP–IUGS–UNESCO project no 329. Palaeontological Institute RAS Publisher, Moscow.

Finetti, I., Bricchi, G., Del Ben, A., Pipan, M., Xuan, Z., 1988. Geophysical study of the Black Sea. Monograph of the Black Sea. Bolletino Geofisica Teorica i Applicata 30 (117–118), 197–324.

Geological map of the region between Caucasus and Crimea Mountains (1956). 1/200 000, Ministry of Geology, USSR (in Russian).

Goushtchenko, O.I., Rebetsky, Y.L., Mikhailova, A.V., Goushtchenko, N.Y., Kuok, L.M., Rassanova, G.V., 1993. The recent regional field of stresses and the mechanism of the lithosphere deformation of seismoactive East-Asia region. EUG VII, Strasbourg. Terra abstract Supplement no. 1 to Terra Nova 5, 259.

Grigor'yants, B.V., Guseyn-Zade, I.G., Mustafayev, M.G., 1981. Structural relationships between Mesozoic and Cenozoic sedimentary complexes in the junction zone between the Crimean Mountains and the Greater Caucasus. Geotectonics 15, 424–432.

Kazantsev, Yu.V., Bekher, N.I., 1988. Allochthonous structures of the Kertch peninsula. Geotectonics 22, 346–355.

Khain, V.E., 1950. Geotektonicheskaya evolyutsiya Yugo-Vostochnogo Kavkaz (Geotectonic evolution of southeastern Caucasus). Baku, Azneftizdat (in Russian).

Khain, V.E., Shardanov, A.N., 1957. Geologic structure of northern slope southeastern Caucasus, Mater. po geol. Severo-Vostochnogo Azerbaizhana (Materials on geology of Northeastern Azerbaidjan). Baku, Akademya, Nauk Azer. SSR (in Russian).

Korotaev, M.V., 1998. Sedimentary basins in compressional environments: modelling of rapid subsidence phases. Ph.D. Thesis, Moscow State University, Moscow, 170 p. (in Russian).

Leonov, M.G., 1985. Diki flysch Alpiiskoi oblasti (Wild flysch of Alpine area). Nauka, Moscow (in Russian).

Letouzey, J., 1986. Cenozoic paleo-stress pattern in the Alpine foreland and structural interpretation in a platform basin. Tectonophysics 132, 215–231.

Maisadze, F.D., 1994. On Upper Eocene olistostromes of southern slope of Greater Caucasus. Geotektonika 2, 95–102 (in Russian).

Mattauer, M., Mercier, J.L., 1980. Microtectonique et grande tectonique. Mémoire hors série de la Société Géologique de France 10, 141–161.

Mercier, J.L., Sorel, D., Simeakis, K., 1987. Changes in the state of stress in the overriding plate of a subduction zone: the Aegean Arc from the Pliocene to the Present. Annale Tectonicae 1, 20–39.

Milanovsky, E.E., 1991. Geology of the USSR, Part 3. Moscow University Press, Moscow 272 pp. (in Russian).

Milanovsky, E.E., 1996. Geology of the Russia and Adjacent Areas (Northern Eurasia). Moscow University Press, Moscow 448 pp. (in Russian).

Milanovsky, E.E., Khain, V.E., 1963. Geologicheskoye Stroenie Kavkaza (Geological Structure of Caucasus). Izdateistvo MGU, Moscow 357 pp. (in Russian).

Muratov, M.V., Tseisler, V.M., 1978. Gornyy Krym i Kerchenskiy poluostrov (Crimean Mountains and Kerch peninsula). In: Tectonics of Europe and Adjacent Regions. Variscide, Epipaleozoic Platforms, and Alps. Explanatory Text to the International Tectonic Map of Europe and Adjacent Regions, scale 1:2 500 000. Izdateistvo Nauka, Moscow, pp. 489–494.

Muratov, M.V., Arkhipov, I.V., Uspenskaya, Y.A., 1984. Structural evolution of the Crimea Mountains and comparison with the Western Caucasus and the Eastern Balkan Ranges. International Geological Review 26, 1259–1266.

Nevesskaya, et al., 1984. Correlation of the eastern–western Para-Tethys and Mediterranean regiostages. In: Popov, S.V. (Ed.), Excursion Guidebook, Neogene Stratigraphy and Palaeontology of the Taman and Kerch peninsulas, Field symposium 4–14th June, 1996, IGCP–IUGS–UNESCO project no 329. Palaeontological Institute RAS Publisher, Moscow, p. 1996.

Nikishin, A.M., Cloetingh, S., Baraboshkin, E.Yu., Bolotov, S.N., Kopaevich, L.F., Nazarevich, B.P., Panov, D.I., Brunet, M.F., Ershov, A.V., Kosova, S.S., Il'ina, V.V., Stephenson, R.A., 1998. Scythian platform, Caucasus and Black Sea region: Mesozoic–Cenozoic tectonic history and dynamics. In: Barrier, E., Crasquin-Soleau, S. (Eds.), Peri-Tethys Memoir 3: Stratigraphy and Evolution of the Peri-Tethyan Platforms, Mémoire du Muséum national d'Histoire naturelle de Paris, 177, pp. 163–176.

Nikishin, A.M., Ziegler, P.A., Panov, D.I., Nazarevich, B.P., Brunet, M.-F., Stephenson, R.A., Bolotov, S.N., Korotaev, M.V., Tikhomirov, P.L., in press. Mesozoic and Cenozoic evolution of the Scythian Platform–Black Sea–Caucasus domain. Peri-Tethyan Rift/ Wrench Basins and Passive Margins, IGCP 369, Peri-Tethys Memoir 6, Mémoire du Muséum national d'Histoire naturelle de Paris.

Robinson, A.G., Rudat, J.H., Banks, C.J., Wiles, R.L.F., 1996. Petroleum geology of the Black Sea. Marine and Petroleum Geology 13, 195–223.

Saintot, A., Angelier, J., Goushtchenko, O., Ilyin, A., Rebetsky, Y., Vassiliev, N., Yakovlev, F., Malutin, S., 1995. Paleostress reconstruction and major structures in Crimea and NW-Caucasus. EUG VIII, Strasbourg. Abstract supplement no. 1 to Terra Nova 7, 269.

Saintot, A., Angelier, J., Ilyin, A., Goushtchenko, O., 1996. In: Paleostress field reconstruction in Crimea and NW-Caucasus. Annual Meeting of Peri-Tethys Program, Amsterdam, 10–11 juin, 1996.

Saintot, A., Angelier, J., Ilyin, A., Goushtchenko, O., 1998. Reconstruction of paleostress fields in Crimea and the NW-Caucasus: relation with major structure. In: Barrier, E., Crasquin-Soleau, S. (Eds.), Peri-Tethys Memoir 3: Stratigraphy

and Evolution of the Peri-Tethyan Platforms, Mémoire du Muséum national d'Histoire naturelle de Paris, 177, pp. 89–112.

Saintot, A., Angelier, J., Chorowicz, J., Ilyin, A., 1999. Mechanical significance of structural patterns identified by remote sensing studies: a multiscale analysis of brittle tectonic structures in Crimea. Tectonophysics. Europrobe Special Volume 313, 187–218.

Shreider, A.A., Kazmin, V.G., Lygin, V.S., 1997. Magnetic anomalies and age of the Black Sea Deep Basins. Geotectonics 31, 54–64.

Spadini, G., Robinson, A.G., Cloetingh, S.A.P.L., 1997. Thermomechanical modeling of Black Sea: basin formation, subsidence and sedimentation. In: Robinson, A.G. (Ed.), Regional and petroleum geology of the Black Sea and surrounding regions, American Association of Petroleum Geologists Memoir, 68, pp. 19–38.

Tugolesov, D.A., Gorshkov, A.S., Meysner, L.B., Solov'yev, V.V., Khakhalev, Ye.M., 1985. The Tectonics of the Black Sea Trough. Geotectonics 19, 435–445.

Wallace, R.E., 1951. Geometry of shearing stress and relation to faulting. Journal of Geology 59, 118–130.

Zonenshain, L.P., Kuzmin, M.I., Natapov, L.M., 1990. Geology of the USSR: a plate tectonics synthesis. In: Page, B.M. (Ed.), Geophysics Geodynamics Series, 21. American Geophysical Union, Washington, DC, p. 242.